

RESEARCH ARTICLE

Radical-free hyperpolarized MRI using endogenously occurring pyruvate analogues and UV-induced nonpersistent radicals

Claudia C. Zanella¹ | Andrea Capozzi¹ | Hikari A. I. Yoshihara¹  |
Alice Radaelli¹  | Adèle L. C. Mackowiak² | Lionel P. Arn² | Rolf Gruetter¹ |
Jessica A. M. Bastiaansen² 

¹Laboratory of Functional and Metabolic Imaging, EPFL, Lausanne, Switzerland

²Department of Diagnostic and Interventional Radiology, Lausanne University Hospital (CHUV) and University of Lausanne (UNIL), Lausanne, Switzerland

Correspondence

Jessica A. M. Bastiaansen, Department of Diagnostic and Interventional Radiology, University Hospital Lausanne (CHUV) and University of Lausanne (UNIL), Rue de Bugnon 46, BH 08.74, 1011, Lausanne, Switzerland.
Email: jbastiaansen.mri@gmail.com

Funding information

Emma Muschamp Foundation; Schweizerische Herzstiftung, Grant/Award Number: FF18054; Schweizerischer Nationalfonds zur Förderung der Wissenschaftlichen Forschung, Grant/Award Numbers: PZ00P3_167871, CRSK-2_190547, PZ00P2_193276

It was recently demonstrated that nonpersistent radicals can be generated in frozen solutions of metabolites such as pyruvate by irradiation with UV light, enabling radical-free dissolution dynamic nuclear polarization. Although pyruvate is endogenous, the presence of pyruvate may interfere with metabolic processes or the detection of pyruvate as a metabolic product, making it potentially unsuitable as a polarizing agent. Therefore, the aim of the current study was to characterize solutions containing endogenously occurring alternatives to pyruvate as UV-induced nonpersistent radical precursors for in vivo hyperpolarized MRI. The metabolites alpha-ketoglutarate (α kV) and alpha-ketobutyrate (α kB) are analogues of pyruvate and were chosen as potential radical precursors. Sample formulations containing α kV and α kB were studied with UV-visible spectroscopy, irradiated with UV light, and their nonpersistent radical yields were quantified with electron spin resonance and compared with pyruvate. The addition of ^{13}C -labeled substrates to the sample matrix altered the radical yield of the precursors. Using α kB increased the ^{13}C -labeled glucose liquid-state polarization to $16.3\% \pm 1.3\%$ compared with $13.3\% \pm 1.5\%$ obtained with pyruvate, and $8.9\% \pm 2.1\%$ with α kV. For $[1-^{13}\text{C}]$ butyric acid, polarization levels of $12.1\% \pm 1.1\%$ for α kV, $12.9\% \pm 1.7\%$ for α kB, $1.5\% \pm 0.2\%$ for OX063 and $18.7\% \pm 0.7\%$ for Finland trityl, were achieved. Hyperpolarized $[1-^{13}\text{C}]$ butyrate metabolism in the heart revealed label incorporation into $[1-^{13}\text{C}]$ acetylcarnitine, $[1-^{13}\text{C}]$ acetoacetate, $[1-^{13}\text{C}]$ butyrylcarnitine, $[5-^{13}\text{C}]$ glutamate and $[5-^{13}\text{C}]$ citrate. This study demonstrates the potential of α kV and α kB as endogenous polarizing agents for in vivo radical-free hyperpolarized MRI. UV-induced, nonpersistent radicals generated in endogenous metabolites enable high polarization without requiring radical filtration, thus simplifying the quality-control tests in clinical applications.

Abbreviations used: α kB, alpha-ketobutyric acid (2-oxobutanoic acid); α kV, alpha-ketoglutaric acid (2-oxopentanoic acid); BA, butyric acid (butanoic acid); DNP, dynamic nuclear polarization; ESR, electron spin resonance; FM, frequency modulation; Glc, glucose; PA, pyruvic acid (2-oxopropanoic acid); SNR, signal-to-noise ratio; TEMPOL, 1-*t*-oxidanyl-2,2,6,6-tetramethylpiperidin-4-ol; TR, repetition time; UV, ultraviolet; UV-Vis, ultraviolet-visible.

This is an open access article under the terms of the Creative Commons Attribution License, which permits use, distribution and reproduction in any medium, provided the original work is properly cited.

© 2021 The Authors. *NMR in Biomedicine* published by John Wiley & Sons Ltd.

KEYWORDS

cardiac metabolism, DNP, endogenous contrast agents, hyperpolarized ^{13}C , metabolism, MRS, nonpersistent radicals, radical-free, UV irradiation

1 | INTRODUCTION

Hyperpolarization via dissolution dynamic nuclear polarization (DNP) can enhance the polarization of nuclear spins by several orders of magnitude.¹ Hyperpolarized ^{13}C -enriched probes have enabled real-time imaging of metabolic pathways in vivo.²⁻⁶ More recently, a successful translation to human subjects was achieved,⁷ demonstrating the potential of hyperpolarized MR for several clinical applications.⁸⁻¹²

Hyperpolarization via DNP requires the presence of polarizing agents, in the form of free radicals, which will transfer their high spin order to the surrounding nuclei upon microwave irradiation at an appropriate frequency. Typically, these free radicals are persistent and added to the sample via chemical doping. Persistent radicals have proven to be highly efficient for dissolution DNP.^{13,14} This poses a challenge for the clinical translation: free radicals may be toxic for living organisms and their presence shortens the brief measurement window of the imaging experiment.^{3,15,16} Employing nonpersistent radicals generated via UV light irradiation of particular precursor molecules may address this challenge. Nonpersistent radicals recombine into diamagnetic and biocompatible species at 190 K¹⁷ and are thereby eliminated instantly during the dissolution process, resulting in radical-free hyperpolarized solutions. This obviates the need for filtration of the endogenous radical precursor.

Several candidates have been demonstrated as suitable precursors for UV-induced nonpersistent radicals, namely a mixture of butanol and phenol,¹⁸ and several α -keto acids such as pyruvic acid (PA),¹⁹⁻²² [2- ^{13}C]PA,²³ phenylglyoxylic acid,²⁴ trimethylpyruvic acid²⁵ and α -ketoisocaproic acid.²⁶ It should be noted that trimethylpyruvic acid is not endogenous and showed great polarization capability only in its in-house synthesized deuterated form.²⁵ To date, a few in vivo studies have demonstrated the use of UV-induced nonpersistent radicals to measure in vivo metabolic processes.^{19,21,24} While phenylglyoxylic acid was demonstrated to be beneficial as a polarizing agent for photosensitive metabolites,²⁴ the achievable polarization levels were relatively low, at least at 3.35 T and 1.25 K. The use of PA as a polarizing agent achieved relatively high polarization levels,¹⁹⁻²² but its presence may interfere or even compete with metabolic processes that involve or are linked to pyruvate dehydrogenase (PDH) activity or the formation of acetyl-CoA.^{6,27-29} For example, while our group has demonstrated the copolarization of [1- ^{13}C]butyrate, a short chain fatty acid, with [1- ^{13}C]pyruvate, using UV-induced nonpersistent radicals,²¹ a prior in vivo hyperpolarized ^{13}C MR study demonstrated that the metabolism of hyperpolarized [1- ^{13}C]butyrate was altered in the presence of PA,⁶ likely due to the acetyl-CoA produced by increased PDH flux. For the above reasons, it is therefore of interest to find off-the-shelf endogenously occurring alternatives to PA for their use as nonpersistent radical precursors. Such alternatives may be advantageous for the measurement of hyperpolarized short- or medium-chain fatty acid metabolism.^{6,30-36} Additionally, such alternatives to PA may be beneficial for hyperpolarized MR studies, where the formation of pyruvate itself is a metabolic product of interest,³⁷⁻³⁹ and can therefore not be coinjected as a radical precursor.

α -ketobutyrate (αkB) and α -ketovalerate (αkV) are two analogues of PA that naturally occur in human blood,^{40,41} but which have different biochemical properties, with their longer side chains making them poorer substrates of the enzymes PDH and lactate dehydrogenase (LDH).⁴¹⁻⁴⁴ For example, αkB was approximately a 50% less efficient substrate of the enzyme PDH compared with PA, while αkV is neither a substrate nor inhibitor of PDH,⁴¹ and unlikely to be a substrate for heart LDH.^{43,44} Because it has been demonstrated that UV irradiation of α -keto acids creates radicals,²⁵ αkB and αkV may have high potential to be used as nonpersistent radical precursors.

The aim of this study was to further expand the field of UV-induced nonpersistent radicals by characterizing the endogenous pyruvate analogues αkV and αkB following UV irradiation and to quantify their potential as endogenous polarizing agents for dissolution DNP. Effects of matrix composition on radical yields and polarization levels of ^{13}C -labeled butyric acid (BA) and glucose (Glc) were quantified and a comparison was made with PA. In a proof-of-concept in vivo study it was investigated whether αkV and αkB could be used to measure cardiac metabolism of ^{13}C -labeled BA.

2 | EXPERIMENTAL

2.1 | Sample formulation and preparation

All chemicals were ordered from Sigma-Aldrich (Buchs, SG, Switzerland). Different sample formulations were used depending on the type of experiment.

Ultraviolet-visible (UV-Vis) spectroscopy experiments were performed at room temperature on 100 mM of αkV , αkB or PA in glycerol-water for characterizing UV light absorption of the radical precursors.

Electron spin resonance (ESR) was used to characterize the ESR line-shape and to quantify the concentration of the photo-induced radicals. ESR experiments were performed with 5 M solutions of α kV, α kB or PA in glycerol: water (1:1, v/v). The ESR signal intensity was calibrated using six glycerol-water solutions with known TEMPOL concentrations between 0 and 100 mM (Figure S1). In a second series of experiments, 2 M unlabeled Glc or 5.7 M BA was added to glycerol-water and the amount of radical precursor was empirically optimized to obtain 40 mM of non-persistent radicals after 200 s of UV irradiation, to ensure comparability of the DNP experiments (see the supporting information for more details on the empirical optimization procedure). Setting the target radical concentration to 40 mM was a choice made based on previous experience with broad line-width radicals used to hyperpolarize ^{13}C -labeled nuclei at 7 T.^{37,45}

Hyperpolarized ^{13}C MRS was performed on samples containing fully deuterated, fully ^{13}C -labeled glucose ($[\text{U-}^{13}\text{C}_6, \text{U-}^2\text{H}_7]\text{Glc}$) or $[1\text{-}^{13}\text{C}]$ butyric acid ($[1\text{-}^{13}\text{C}]\text{BA}$). After optimization on samples prepared with nonlabeled compounds, the amount of radical precursor was set to 5.7 M α kV, 4.1 M α kB and 1.6 M PA for samples containing $[\text{U-}^{13}\text{C}_6, \text{U-}^2\text{H}_7]\text{Glc}$. Conversely, the radical precursor was set to 2.4 M α kV and 4.0 M α kB for samples containing $[1\text{-}^{13}\text{C}]\text{BA}$. The latter were also used for in vivo measurements.

To compare liquid-state polarization levels obtained with persistent trityl radicals, $[1\text{-}^{13}\text{C}]\text{BA}$ was hyperpolarized using OX063 by adjusting a previously published recipe^{31,34} by increasing the radical concentration to 25 mM without adding a Gd-based contrast agent. Additionally, based on the poor performance of OX063 and to compare with a matrix formulation used for the UV-induced nonpersistent radical measurements, Finland trityl acid was added to a final concentration of 25 mM to the $[1\text{-}^{13}\text{C}]\text{BA} + \alpha$ kB sample formulation (without performing UV irradiation).

2.2 | Creating nonpersistent radicals on metabolites using UV irradiation

To create nonpersistent radicals, the sample formulations described in the previous section were sonicated and degassed at 50°C for 20 min prior to pipetting 6- μl droplets and freezing them in liquid nitrogen to create a solid pellet. The pellets were transferred to a quartz Dewar (Magnetech, Freiberg Instruments, Germany) filled with liquid nitrogen and irradiated with a broadband UV lamp (Dymax BlueWave 200, Torrington, CT, USA) at maximum power (40 Wcm^{-2}) for a maximum of 200 s using a home-built irradiation setup.²²

In experiments aiming to investigate the time course of radical generation for α kV, α kB or PA ($n = 3$, each precursor), frozen beads were irradiated for a set duration (i.e. 20, 45, 70, 110, 150 and 200 s), and ESR was measured at the end of each step.

2.3 | Quantification and characterization of nonpersistent radicals

UV-Vis spectroscopy was performed to measure the light absorbance of the different radical precursors using a single beam UV-3100PC spectrophotometer (VWR International) and a 1-mm pathlength quartz cuvette. UV light absorption of 100 mM α kV, α kB or PA in glycerol-water samples was measured from 280 to 600 nm in steps of 0.5. Measurements were performed at room temperature because there was no significant difference between the absorbance spectra of PA solutions acquired at room and liquid-nitrogen temperatures.²²

ESR was used to determine the nonpersistent radical concentration generated in the samples after UV irradiation at liquid-nitrogen temperature. X-band ESR was performed at 77 K as well using a MiniScope MS 400 spectrometer (Magnetech GmbH, Germany). Spectrometer parameters were chosen to ensure that saturation of the ESR signal was avoided over the entire range of radical concentrations and kept constant throughout all experiments. Parameters were set to: 20 s sweep time, 20 mT magnetic field range, 0.2 mT magnetic field modulation amplitude and 30 dB power attenuation. The ESR experiments were performed on two 6- μl beads for each sample formulation. Subsequently, the beads were extracted from the quartz Dewar and transferred to a preweighed microcentrifuge tube, which was then weighed to determine their exact volume and correct the concentration calibration.

2.4 | Hyperpolarization via DNP

All DNP experiments were performed in a 7-T custom-built polarizer. Nuclear spins were hyperpolarized using a millimeter-wave source centered at 197 GHz, with digital control for frequency modulation (FM), a 55-mW output power and a 1-GHz tuning range (Elva-1 VCOM-06/197/1.0/55-DD). Experiments were performed to determine the optimal hyperpolarization conditions in terms of microwave irradiation frequency and to quantify polarization build-up times. The microwave frequency sweeps were performed with and without microwave FM to find the optimal DNP conditions and to quantify the effect of microwave FM on the enhancement. The sample cup was filled with 12 frozen UV-irradiated beads containing $[\text{U-}^{13}\text{C}, \text{U-}^2\text{H}]\text{Glc}$. Microwave frequency-modulated profiles were acquired at 4.2 K using a constant 40 MHz modulation amplitude and 5 kHz modulation rate for each microwave frequency step. The step size was 40 MHz for beads containing α kV or α kB, and 20 MHz for beads containing PA. For each frequency step, the sample was irradiated for 40 min and the polarization build-up was monitored using hard 2° RF excitation pulses every 5 min. FM was not used, either for Finland trityl or for Ox063 samples.

The optimal conditions found in the previous experiments for a given set of FM parameters were used to hyperpolarize [U-¹³C, U-²H]Glc as well as [1-¹³C]BA for quantification of ¹³C polarization levels in liquid state after dissolution and for the in vivo experiments. The ¹³C-labeled metabolites were hyperpolarized at 1.05 ± 0.02 K for 2.5 h, with frequency-modulated (40 MHz amplitude at a rate of 5 kHz) microwave irradiation at 196.69 GHz center frequency for αkV and αkB, and at 196.65 GHz center frequency for PA. Their polarization build-up was monitored using 2° RF excitation pulses every 5 min.

2.5 | Dissolution DNP, hyperpolarized ¹³C MRS in phantoms and in vivo

Frozen hyperpolarized beads were dissolved using either 5.5 ml of D₂O or a phosphate buffered saline solution for liquid-state in vitro and in vivo experiments, respectively.^{45,46} The dissolved sample was automatically transferred to a separator/infusion pump located in a 9.4-T horizontal bore magnet (Agilent, Palo Alto, CA, USA).⁴⁷ Hyperpolarized ¹³C MR spectra were recorded within the pump using a dual ¹H/¹³C volume coil starting 3 s after dissolution and using a 5° RF excitation pulse with 3 s repetition time (TR). After a complete decay of the hyperpolarized magnetization, a thermal equilibrium ¹³C spectrum of the sample was acquired using a 90° RF excitation pulse, with a TR of 60 s and 64 averages. The enhancement ϵ was calculated as the ratio of the hyperpolarized and thermal signal peak integral, taking into account a correction for the RF excitation angle and the number of averages. The remaining ¹³C hyperpolarization after dissolution and transfer was calculated as $P = \epsilon * \tanh\left(\frac{h\nu_C B_0}{2k_B T}\right)$, where the hyperbolic tangent represents the ¹³C thermal equilibrium polarization at 293 K and 9.4 T.

In vivo experiments were performed on two male Wistar rats (one injection each) to demonstrate the feasibility of the novel polarizing agents to measure the cardiac metabolism of hyperpolarized [1-¹³C]BA, and to obtain preliminary information on in vivo chemical shifts. The feasibility study was conducted according to federal ethical guidelines and was approved by the local regulatory body. Anesthesia protocols and physiological monitoring were described previously.^{6,21} A volume of 62-μl [1-¹³C]BA was hyperpolarized, similar to our prior work,^{6,21} with procedures described in the previous section. Frozen droplets of 10 M NaOH solution were added to the sample cup to neutralize the hyperpolarized solution during dissolution. Following an automated dissolution and transfer to the separator infusion pump,⁴⁷ which was prefilled with 0.6 ml of phosphate buffered saline and heparin, 0.8 ml of the hyperpolarized solution was administered via a femoral vein catheter.

MR data were recorded using a custom-made RF hybrid probe of ¹H/¹³C-pair surface coils placed on the chest of the animal in supine position. Correct positioning of the coil on top of the heart was ensured using gradient echo ¹H MRI. FAST (EST)MAP shimming was performed until a ¹H linewidth of 30 Hz was achieved. Respiratory-gated and cardiac-triggered unlocalized MR acquisitions were performed using a ¹H-decoupled (WALTZ-16)⁴⁸ sequence with adiabatic 30° RF excitation pulses (BIR-4)⁴⁹ and a TR of 3 s. Free induction decays consisting of 8258 complex data points were acquired to sample a bandwidth range of 20.5 kHz. The first spectra acquired following injection, in which metabolic products were absent, were used to confirm the resonances identified in phantom experiments (Figure S2).

2.6 | Data processing and analysis

The ESR concentration calibration curve was obtained from fitting the second integrals of the ESR signal intensity linearly as a function of the radical concentration (Figure S1). To calculate the build-up rate of nonpersistent radical formation, the second integral of the ESR signal intensity was corrected for bead volume variation prior to performing an intensity calibration to quantify absolute concentrations.

Following methods previously described,²² the radical generation time course was fit to a monoexponential function to extract the radical generation rate constant and plateau value.

Regarding the DNP sweeps, the y-axis value at each frequency point corresponded to the polarization plateau measured at 4.2 K. The non-modulated sweeps were normalized to 1 and the relative increase in DNP enhancement due to microwave modulation was then calculated accordingly. The microwave frequencies at which the highest polarization levels are achieved are referred to as the negative DNP maximum and the positive DNP maximum.

For each sample, the polarization time course at the best DNP condition was fit to a monoexponential function to extract the build-up time constant and the polarization plateau, as is customary. Accordingly, each sample was irradiated for at least three time constants prior to dissolution.

Statistically significant differences between polarization levels obtained using αkB or αkV compared with PA were tested via an unpaired, two-tail t-test assuming equal variance, with *p* less than 0.05 considered significant.

In vivo spectra were postprocessed in VnmrJ 3.2 (Agilent, Palo Alto, CA, USA) using 20 Hz line-broadening, baseline correction and drift correction. The signal-to-noise ratio (SNR) was calculated as the ratio of the highest signal intensity after phasing and the standard deviation of the noise over a region without metabolic or injected substrate resonances. All in vivo spectra where the [1-¹³C]acetylcarnitine resonance was visible were summed, corresponding to 10 consecutive spectra in the case of αkV, and 12 spectra in the case of αkB. Chemical shifts were assigned using [1-¹³C]acetylcarnitine as the reference peak resonating at 173.9 ppm and assigning all other metabolites as indicated before.⁶

3 | RESULTS

To characterize structural changes and absorption characteristics of UV-light irradiation on the metabolites α kV, α kB and PA, UV-Vis spectroscopy and ESR measurements were performed: UV-Vis absorption spectra showed an ~ 1.7 -fold higher absorbance for α kV compared with α kB or PA (Figure 1A). α kB and PA showed nearly identical absorbance maxima in the UV range of 300–400 nm (Figure 1A). Absorbance of all three metabolites peaked at around a wavelength of 320 nm.

ESR performed on frozen samples prior to UV irradiation indicated the initial absence of unpaired electron spins in the matrixes of glycerol-water mixed with 5 M of α kV, α kB or PA. ESR spectra acquired after 200 s of UV irradiation demonstrated that free radicals were generated within the frozen samples (Figure 1B–D). ESR spectra of α kV and α kB showed a nearly identical shape (Figure 1B,C), but were distinct from the PA spectrum (Figure 1D). The production of nonpersistent radicals as a function of UV-irradiation time followed a near monoexponential build-up (Figure 1E) with a characteristic time constant of 30.9 ± 5.1 s for α kV, 37.0 ± 5.2 s for α kB and 46.5 ± 1.4 s for PA (Table 1). The maximum

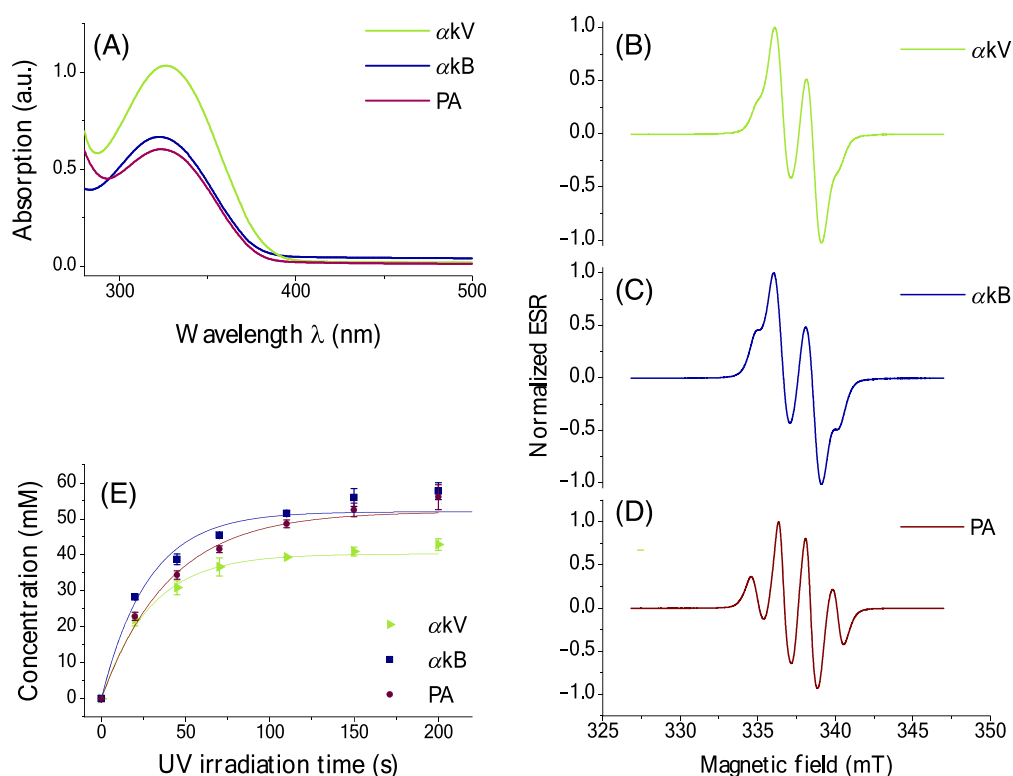


FIGURE 1 Ultraviolet-visible (UV-Vis) absorption spectra at room temperature and X-band electron spin resonance (ESR) at 77 K. (A) UV-Vis absorption spectra of 100 mM radical precursor in glycerol-water using a 1 mm light path showing UV-light absorbance of alpha-ketovaleric acid (α kV), alpha-ketobutyric acid (α kB) and pyruvic acid (PA). (B–D) ESR spectra of the endogenous metabolites α kV, α kB and PA at 77 K after 200 s of UV irradiation with a 40 W cm^{-2} power UV-light source. (E) Radical concentration build-up curves of 5 M precursor in glycerol-water upon UV irradiation. Table 1 lists corresponding build-up times and maximum radical concentrations

TABLE 1 UV-induced radical build-up times and maximum nonpersistent radical concentrations obtained after 200 s of UV irradiation in formulations containing 5 M precursor dissolved in glycerol-water. Data were acquired at 77 K using X-band electron spin resonance. Build-up rates were calculated from fitting a monoexponential function to the radical concentration build-up curves (Figure 1E). Values represent mean and standard deviation, $n = 3$

	Build-up time (s)	Maximal concentration (mM)
α kV	30.9 ± 5.1	41.6 ± 0.6
α kB	37.0 ± 5.2	56.1 ± 2.7
PA	46.5 ± 1.4	55.0 ± 1.9

Abbreviations: α kB, alpha-ketobutyric acid; α kV, alpha-ketovaleric acid; PA, pyruvic acid.

nonpersistent radical concentrations were 41.6 ± 0.6 mM for α kV, 56.1 ± 2.7 mM for α kB and 55.0 ± 1.9 mM for PA (Figure 1E). Irradiating the samples for 200 s resulted in plateauing the radical concentration while avoiding pulverization of the beads due to excessive UV irradiation.

To obtain transparent glassy beads that remained intact upon irradiation with UV light, 2 M Glc was dissolved with glycerol-water and admixed with 5.7 M α kV, 4.1 M α kB or 1.6 M PA. These formulations yielded a nonpersistent radical concentration of 41.5 ± 2.5 mM in α kV, 39.5 ± 2.3 mM in α kB and 41.7 ± 2.0 mM in PA after 200 s of UV irradiation (Figure 2A).

To assess the effect of FM of the microwave irradiation, the ^{13}C nuclear polarization was measured as a function of the microwave frequency, which for the α kV and α kB sweeps showed a broadening when FM was applied. FM improved the DNP performance in terms of signal enhancement of hyperpolarized ^{13}C -labeled Glc by 100%, 50% and 30% for α kV, α kB and PA, respectively (Figure 3, Table 2). For α kV and α kB/PA, the microwave frequencies of the positive and negative DNP maxima were observed at $\nu_{\max} = 196.69/196.65$ GHz and $\nu_{\min} = 196.89/196.89$ GHz, respectively (Figure 3, Table 2).

To determine the build-up rates of nuclear magnetization, the latter was measured as a function of microwave irradiation duration. The solid state build-up times of hyperpolarized $[\text{U-}^{13}\text{C}, \text{U-}^2\text{H}]\text{Glc}$ were 1.7 ± 0.5 , 1.3 ± 0.5 and 1.6 ± 0.5 ks for α kV, α kB and PA, respectively (Table 3).

Following dissolution, the liquid-state polarization for the C_{2-5} group of $[\text{U-}^{13}\text{C}, \text{U-}^2\text{H}]\text{Glc}$ was $8.9\% \pm 2.1\%$, $16.3\% \pm 1.3\%$ and $13.1\% \pm 1.5\%$ for α kV, α kB and PA, respectively (Table 3, Figure 4). While $[\text{U-}^{13}\text{C}, \text{U-}^2\text{H}]\text{Glc}$ hyperpolarized with α kB showed significantly higher liquid-state polarization than that hyperpolarized using PA ($p = 0.048$), there was no significant difference between PA and α kV ($p = 0.09$). The quantification of polarization levels on the C_1 and C_6 resonances of Glc did not alter the results (Table 3).

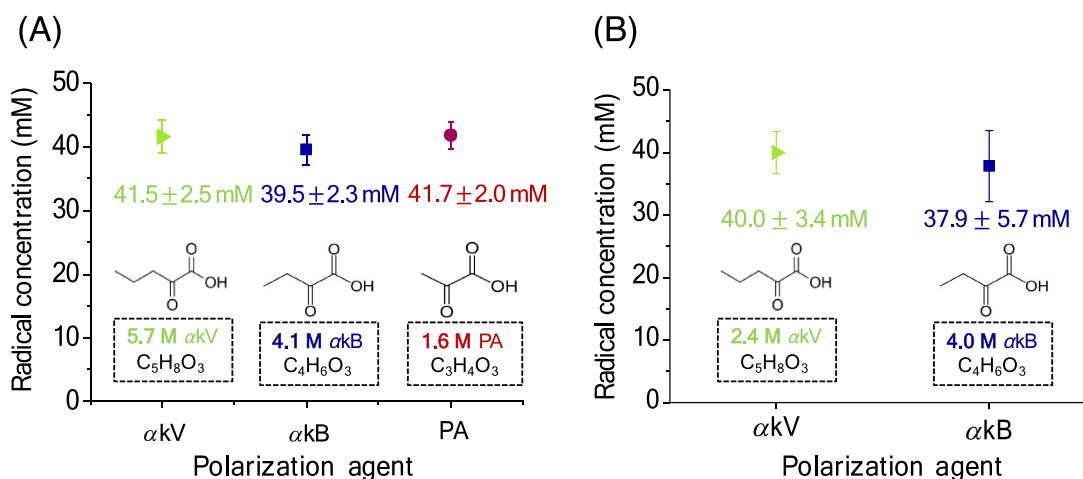


FIGURE 2 Sample formulations were optimized to obtain ~ 40 mM of nonpersistent radicals after 200 s of UV irradiation in (A) $[\text{U-}^{13}\text{C}, \text{U-}^2\text{H}]\text{glucose}$ and (B) $[\text{1-}^{13}\text{C}]\text{butyric acid}$. Underlying chemical structures are illustrated for each nonpersistent radical precursor, with the required concentrations indicated

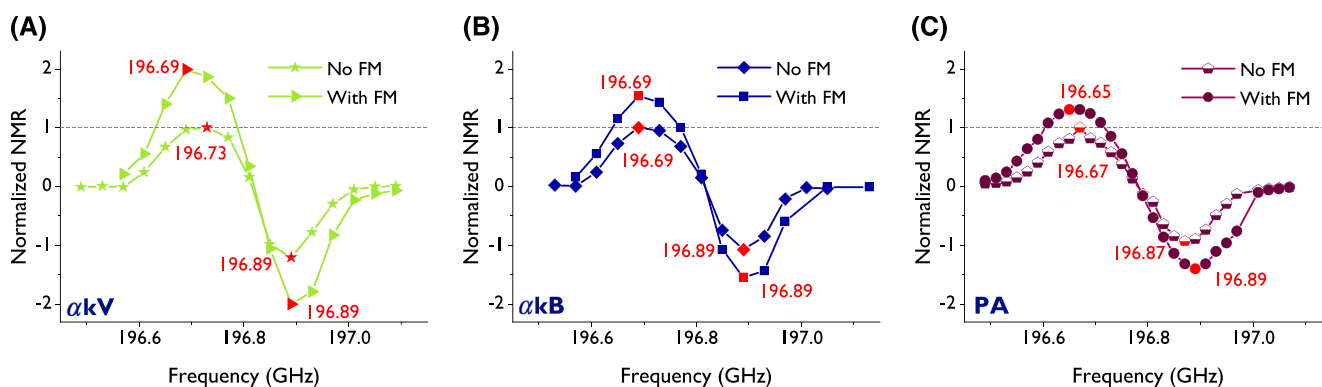


FIGURE 3 Hyperpolarized ^{13}C signal as a function of microwave frequency with and without the application of frequency modulation (FM). Formulations containing $[\text{U-}^{13}\text{C}, \text{U-}^2\text{H}]\text{Glc}$ in glycerol-water were hyperpolarized at 7 T and 4.2 K. FM was set to 40 MHz amplitude at a frequency of 5 kHz. Microwave frequencies corresponding to observed dynamic nuclear polarization (DNP) maxima and minima are reported (numbers in red) in Table 2. Hyperpolarization was achieved using the UV radicals (A) alpha-ketovaleric acid (α kV), (B) alpha-ketobutyric acid (α kB) and (C) pyruvic acid (PA)

TABLE 2 Microwave center frequencies at which dynamic nuclear polarization (DNP) maxima and minima occur at 7 T. Microwave frequency sweeps (Figure 3) were conducted on [U-¹³C, U-²H]Glc in glycerol-water samples. The microwave frequency was swept using either monochromatic microwave irradiation or frequency modulation with 40 MHz modulation amplitude at a 5 kHz rate

	Microwave frequency modulation	Positive DNP maximum (GHz)	Negative DNP maximum (GHz)
α kV	no	196.73	196.89
	yes	196.69	196.89
α kB	no	196.69	196.89
	yes	196.96	196.89
PA	no	196.67	196.87
	yes	196.65	196.89

Abbreviations: α kB, alpha-ketobutyric acid; α kV, alpha-ketovaleric acid; PA, pyruvic acid.

TABLE 3 Polarization build-up time constants at 7 T, 1.05 ± 0.02 K and liquid-state polarization levels of the C₁, C_{2–5} and C₆ resonances of [U-¹³C₆, U-²H₇]Glc at 9.4 T, 20°C. Liquid-state enhancement was calculated as a ratio of hyperpolarized signal (rectangular RF excitation pulse of duration $\tau = 5 \mu$ s, RF excitation angle $\alpha = 5^\circ$) and thermal signal (64 averages of $\alpha = 90^\circ$ with $\tau = 90$ s, TR = 60 s). Values show mean and standard deviation over $n = 3$ datasets

$n = 3$	Build-up time (s)	C ₁ Glc liquid-state polarization (%)	C _{2–5} Glc liquid-state polarization (%)	C ₆ Glc liquid-state polarization (%)
α kV	1.7 k \pm 0.5 k	9.4 \pm 3.0	8.9 \pm 2.1	8.0 \pm 2.8
α kB	1.3 k \pm 0.5 k	16.8 \pm 0.4	16.3 \pm 1.3	14.6 \pm 1.7
PA	1.6 k \pm 0.5 k	13.9 \pm 1.8	13.3 \pm 1.5	11.5 \pm 2.5
Conditions	7 T, 1.05 K	9.4 T, 293 K		

Abbreviations: α kB, alpha-ketobutyric acid; α kV, alpha-ketovaleric acid; PA, pyruvic acid.

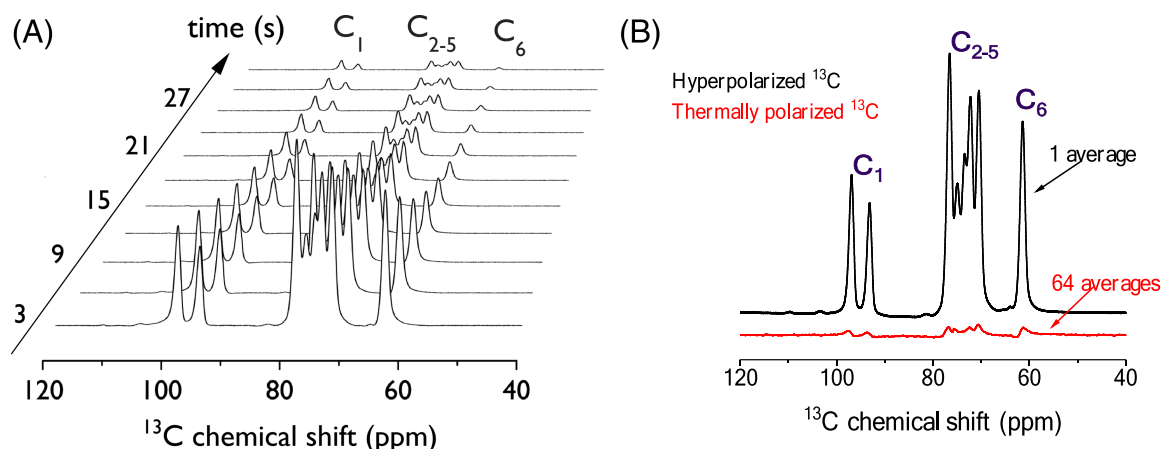


FIGURE 4 Hyperpolarized ¹³C MRS of [U-¹³C, U-²H]glucose (Glc) sample formulations. (A) Liquid-state ¹³C signal evolution of [U-¹³C, U-²H] Glc hyperpolarized using alpha-ketobutyric acid (α kB) as a polarizing agent. (B) Hyperpolarized ¹³C MR spectrum of [U-¹³C, U-²H]Glc acquired 3 s after dissolution (top) and the thermally polarized ¹³C spectrum (bottom). Acquisitions were performed at 9.4 T and 20°C

The solid state build-up times of hyperpolarized [1-¹³C]butyrate were 2.1 ± 0.3 and 3.3 ± 0.4 ks when hyperpolarized using α kV and α kB, respectively, and 0.8 ± 0.3 and 1.7 ± 0.3 ks for OX063 and Finland trityl radicals, respectively. Liquid-state enhancement over thermal polarization at 9.4 T was $14.6 \text{ k} \pm 1.4 \text{ k}$ and $15.6 \text{ k} \pm 1.7 \text{ k}$ for the α kV and α kB samples, respectively, which translated to liquid-state polarization of $12.1\% \pm 1.1\%$ and $12.9\% \pm 1.7\%$ (Table 4). The liquid-state polarization for OX063 and Finland trityl was $1.5\% \pm 0.2\%$ and $18.7\% \pm 0.7\%$, respectively. In these experiments, the natural abundance ¹³C resonances of α kV and α kB could be identified as [1-¹³C] α kV (at 172.9 ppm), [1-¹³C] α kV-hydrate (at 180.7 ppm), [2-¹³C] α kV (at 209.1 ppm), [1-¹³C] α kB (at 171.9 ppm), [1-¹³C] α kB-hydrate (at 180.6 ppm) and [2-¹³C] α kB (at 208.4 ppm) (Figure 5). Note that pH was not neutralized in these experiments, and the chemical shifts were different in the pH-neutralized in vivo experiments (Table 5).

TABLE 4 Solid state build-up times at 7 T, 1.05 K are reported for $[1-^{13}\text{C}]$ butyrate samples containing alpha-ketovaleric acid (αkV) or alpha-ketobutyric acid (αkB) as nonpersistent radical precursors, and OX063 and Finland trityl as persistent radicals. Room-temperature liquid-state enhancements and liquid-state polarization were calculated after sample dissolution and transfer to a 9.4-T MR scanner. Mean and average values are obtained from n datasets. Exemplary spectra for the nonpersistent radical samples are shown in Figure 5

Radical	Build-up time (s)	n	Liquid-state enhancement	BA liquid-state polarization (%)	n
αkV	$2.1\text{ k} \pm 0.3\text{ k}$	4	$14.6\text{ k} \pm 1.4\text{ k}$	12.1 ± 1.1	3
αkB	$3.3\text{ k} \pm 0.4\text{ k}$	5	$15.6\text{ k} \pm 1.7\text{ k}$	12.9 ± 1.7	3
Trityl OX063	$0.8\text{ k} \pm 0.3\text{ k}$	3	$1.8\text{ k} \pm 0.2\text{ k}$	1.5 ± 0.2	3
Finland Trityl	$1.7\text{ k} \pm 0.3\text{ k}$	3	$22.7\text{ k} \pm 0.8\text{ k}$	18.7 ± 0.7	3
Conditions	solid state: 7 T, 1.05 K		liquid state: 9.4 T, 293 K		

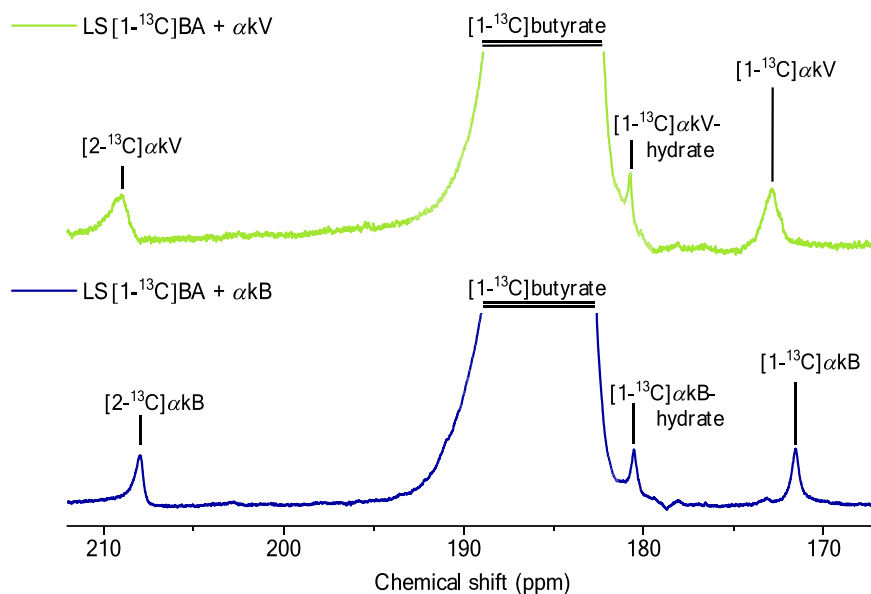


FIGURE 5 Liquid-state ^{13}C MR spectra of $[1-^{13}\text{C}]$ butyrate hyperpolarized using alpha-ketovaleric acid (αkV) (top) and alpha-ketobutyric acid (αkB) (bottom) displaying the ^{13}C -labeled substrate and precursor resonances. Spectra were acquired 3 s postdissolution and were line-broadened with 2 Hz. Solutions were acidic because pH neutralization was not performed in these experiments

TABLE 5 Chemical shifts of observed metabolites in the heart after injection of pH-neutralized hyperpolarized $[1-^{13}\text{C}]$ butyrate in vivo using either alpha-ketovaleric acid (αkV) or alpha-ketobutyric acid (αkB) as a polarizing agent (in vivo spectra are displayed in Figure 6). $[1-^{13}\text{C}]$ acetylcarnitine was used as the reference peak (*) and assigned to 173.9 ppm. The resonance of natural abundance $[1-^{13}\text{C}]$ αkV -hydrate was not detected in these experiments (see also Figure S2)

Metabolite	Chemical shift (ppm)
natural abundance $[2-^{13}\text{C}]$ αkB	209.3
natural abundance $[2-^{13}\text{C}]$ αkV	208.7
$[1-^{13}\text{C}]$ butyrate	184.8
$[5-^{13}\text{C}]$ glutamate	182.4
$[5-^{13}\text{C}]$ citrate	179.8
natural abundance $[1-^{13}\text{C}]$ αkB -hydrate	178.1
$[1-^{13}\text{C}]$ butyrylcarnitine	176.4
$[1-^{13}\text{C}]$ acetoacetate	176.0
$[1-^{13}\text{C}]$ acetylcarnitine	173.9*
natural abundance $[1-^{13}\text{C}]$ αkB	172.1
natural abundance $[1-^{13}\text{C}]$ αkV	172.0

To assess the potential to measure cardiac metabolism, hyperpolarized $[1-^{13}\text{C}]$ butyrate was injected in male Wistar rats. For the first few seconds after injection of the hyperpolarized solution, metabolic products were not observable, and the detected ^{13}C resonances could be identified as $[1-^{13}\text{C}]$ butyrate (at 184.8 ppm), and natural abundance resonances of $[1-^{13}\text{C}]\alpha\text{KV}$ (at 172.0 ppm), $[2-^{13}\text{C}]\alpha\text{KV}$ (at 208.7 ppm), $[1-^{13}\text{C}]\alpha\text{KB}$ -hydrate (at 178.1 ppm), $[1-^{13}\text{C}]\alpha\text{KB}$ (at 172.1 ppm) and $[2-^{13}\text{C}]\alpha\text{KB}$ (at 209.3 ppm). The resonance of $[1-^{13}\text{C}]\alpha\text{KV}$ -hydrate was not detected in vivo, further evidenced by its absence immediately after injection (Figure S2). Maximum in vivo SNR on ^{13}C BA was observed 12 s after dissolution, with an SNR of 1370 for αKV and 1780 for αKB . Cardiac metabolism of hyperpolarized $[1-^{13}\text{C}]$ BA (Figure 6, Table 5) resulted in ^{13}C -labeling of $[1-^{13}\text{C}]$ acetylcarnitine (173.9 ppm), $[1-^{13}\text{C}]$ acetoacetate (176.0 ppm), $[1-^{13}\text{C}]$ butyrylcarnitine (176.4 ppm), $[5-^{13}\text{C}]$ glutamate (182.4 ppm) and $[5-^{13}\text{C}]$ citrate (179.8 ppm). Due to the shoulder of the nearby αKB -hydrate resonance, $[5-^{13}\text{C}]$ citrate could not be detected in the αKB experiment.

4 | DISCUSSION

This study shows that αKV and αKB can be used to generate nonpersistent radicals for hyperpolarizing ^{13}C -labeled substrates, expanding the field of research on radical-free dissolution DNP performed on mixtures containing only endogenously occurring substances. Their potential as polarizing agents for in vivo metabolic studies was also shown in proof-of-concept experiments performed in the heart.

Although UV-irradiated αKV and αKB demonstrated virtually identical ESR line-shapes, their reaction to UV light visibly differed (Figure 1). This was not only seen in the different UV-Vis absorption at 100 mM but also in their different radical yield at 5 M. The likely reason why αKV shows considerably higher absorption compared with αKB and PA, but lower maximum radical concentration, can be ascribed to the fact that UV light cannot efficiently penetrate through the bead volume, with a high precursor concentration. Adding Glc or BA further changed the reaction

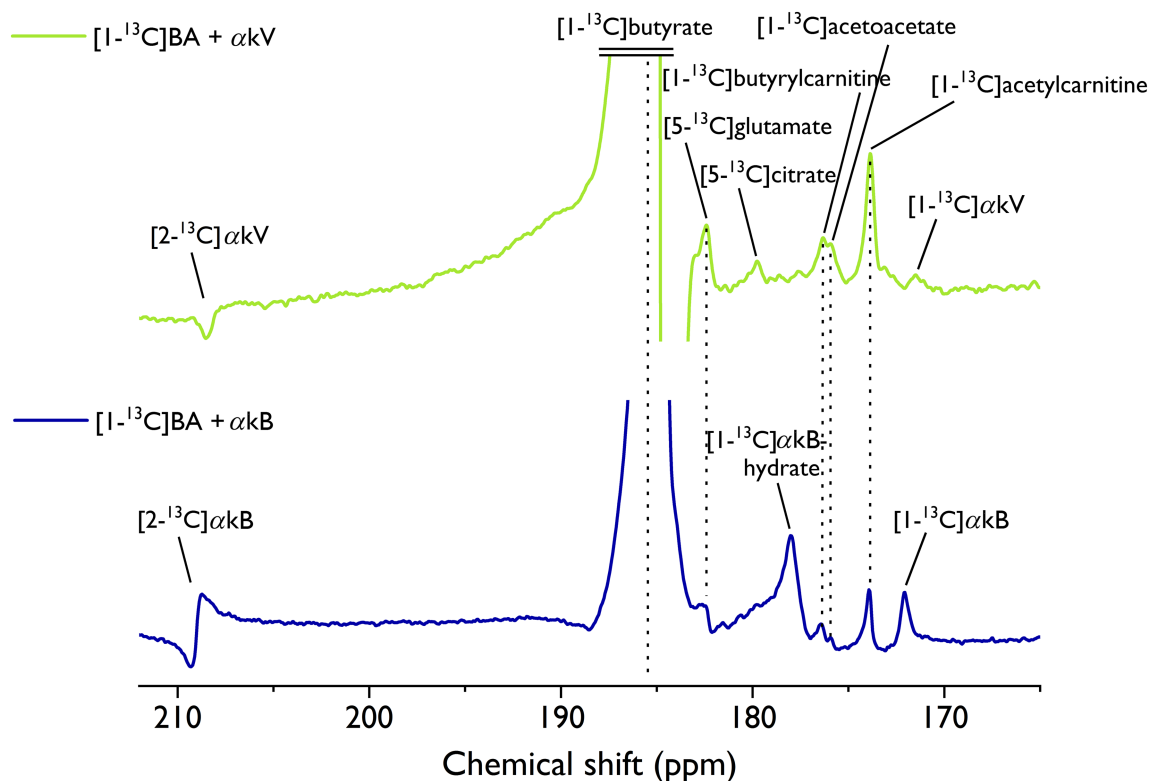


FIGURE 6 In vivo spectra of cardiac metabolism in two male Wistar rats following the injection of a radical-free hyperpolarized $[1-^{13}\text{C}]$ butyrate solution. Hyperpolarization via dynamic nuclear polarization (DNP) was performed at 7 T, 1.05 K using the UV-induced nonpersistent radicals alpha-ketovaleric acid (αKV) (top) and alpha-ketobutyric acid (αKB) (bottom). Spectra where $[1-^{13}\text{C}]$ acetylcarnitine resonances were visible were summed and line-broadened by a factor of 20. Therefore, spectra acquired at 24–51 s (αKV) and 18–51 s postdissolution (αKB) were summed. Cardiac metabolism resulted in the detection of $[1-^{13}\text{C}]$ acetylcarnitine, $[1-^{13}\text{C}]$ acetoacetate, $[1-^{13}\text{C}]$ butyrylcarnitine and $[5-^{13}\text{C}]$ glutamate. $[5-^{13}\text{C}]$ citrate could not be detected in the αKB experiment, due to the proximity and phase of the αKB -hydrate resonance. The natural abundance resonances of the injected precursors αKB and αKV were also identified. The butyrate resonance in the experiment with αKV was distorted by motion or flow. Similarly, the $[2-^{13}\text{C}]\alpha\text{KB}$ peak could not be brought into phase with the other resonances using first-order correction

of each compound to UV light such that a specific sample formulation was required to achieve the targeted nonpersistent radical concentration of 40 mM. As has been observed before,²² the relationship between nonpersistent radical yield and the concentration of the precursor was nonlinear. This posed a challenge during sample formulation optimization. Even although α kV, α kB and PA differ from each other by additional methylene units on their aliphatic side chain, the results from our experiments illustrate that sample formulation requires a careful optimization in terms of UV-induced radical yield and polarization level for each ¹³C-labeled metabolic substrate, which is an empirical and nontrivial process. Because the current work focused on the feasibility of α kV and α kB as nonpersistent radical precursors, optimization of the sample formulation did not go beyond obtaining the targeted concentration of 40 mM nonpersistent radicals, resulting in relatively large concentrations of precursor compared with PA in the ¹³C-labeled sample formulations. It is important to point out that the samples were not specifically optimized to maximize radical yield, to minimize precursor concentrations or to maximize achievable polarization levels, which is a limitation of our study. The empirical approach of optimizing sample formulations, plus the observation that radical quantum yields were comparable in glycerol-water mixtures (Figure 1), show that there is significant room for improvement. Our experience with UV-irradiated nonpersistent radical precursors and published work^{21,22} indicate that precursor volumes can be reduced when boosting radical yield or UV-light penetration, which may be achieved by using different glassing agents such as ethanol, by deuteration of the radical precursors, by changing the relative ratios of precursor to glassing agent, by adapting the UV-irradiation time, or by changing the bead size.

The nuclear polarization levels increased when applying microwave FM, which is a consequence of the relatively broad radical ESR spectrum and short electron T_1 characterizing the UV-radical family (~ 100 ms).^{50–52} By contrast, microwave FM has little effect on narrow linewidth radicals and radicals with long electron T_1 such as OX063 at 6.7 T.⁵³ Similarly, for polarizer systems operating at low field (~ 3.35 T), microwave FM may be less effective because of longer radical T_1 and more narrow spectral width (less g -anisotropy). Microwave FM is a feature that is available on commercially available polarizers working at high field (e.g. the Spin Aligner polarizer; Polarize, Copenhagen, Denmark). Polarization levels in the current study were of the order of 9% to 16% for Glc and 13% for BA, close to the polarization of 18.7% measured when adding Finland trityl to a non-UV-irradiated α kB BA mixture. The recipe for OX063 did not perform as expected on our system based on the low polarization ($\sim 2\%$) that was obtained. This can be a consequence of the apolar nature of the BA sample formulation. Indeed, OX063 is very soluble in polar solvents such as water (log P of -0.5 and -1.38 , respectively). Differently, BA has a log P of 0.79. Most likely, OX063 in the presence of BA made a suspension rather than a solution. The opposite reasoning applies to Finland trityl. In previous work using similar experimental conditions, UV-irradiated metabolite mixtures containing ¹³C-labeled PA and BA were hyperpolarized to significantly lower levels (i.e. $3.3\% \pm 0.5\%$ – $5.2\% \pm 0.5\%$ for ¹³C BA).²¹ The latter was a consequence of a different UV-light source, yielding a third of the radical concentration measured in this study, and the absence of microwave FM.²¹ In the current study, a broadband UV-light source was used, delivering 40 times more power, and glycerol-water was added to the mixtures to improve the DNP sample matrix. Although performed under different experimental conditions and using different methods to calculate the liquid-state polarization, previous studies reported polarization levels of between $22.2\% \pm 2.1\%$ ⁵⁴ and $30.1\% \pm 1.8\%$ ²⁵ for Glc and of between $7\% \pm 2\%$ ³¹ and $28\% \pm 4\%$ ³⁴ for BA. The current results are within a similar range and thus are promising. Although a dedicated optimization in terms of polarization level was not performed in the current study, polarization levels may be further increased by optimization of the sample formulation (i.e. components, concentrations and bead size), or by a detailed investigation of the microwave FM. However, previously reported improvements in DNP performance may conflict with the UV performance and nonpersistent radical generation: for example, using dimethyl sulfoxide as the glassing agent increased the DNP performance by 18-fold when polarizing ¹³C-labeled BA.³⁴ However, UV-Vis spectroscopy and ESR measurements have shown the photosensitive nature of dimethyl sulfoxide and its unsuitability as a glassing agent for UV-induced nonpersistent radical formulations using a broadband UV source.²⁴

Hyperpolarized BA has been used before as a probe to study short-chain fatty acid cardiac metabolism,^{6,21,31,34,35} with different results in terms of the amount of observed metabolites. In the current study, hyperpolarization of BA with α kV and α kB reached sufficient SNR to observe cardiac metabolism, with a similar metabolic profile observed in previous studies using persistent radicals at high magnetic field.^{6,31} High magnetic field allows for a better spectral resolution and thus may facilitate the resolved detection of metabolites such as ¹³C-labeled citrate and glutamate. However, B_0 inhomogeneities also increase, which may complicate shimming procedures, especially around the moving heart, which may result in distorted line shapes and difficult-to-phase spectra. In the current study, the citrate resonance could not be reliably detected due to the shoulder of the neighboring $[1-^{13}\text{C}]\alpha\text{kB}$ -hydrate resonance. Conversely, the absence of $[1-^{13}\text{C}]\alpha\text{kV}$ -hydrate (Figure 6) enabled citrate detection when using α kV. Note that the relative amount of α kV in the BA sample formulation was much smaller compared with the amount of α kB, which contributed to increased signal intensities of natural abundance α kB resonances compared with those of α kV. This can be appreciated when observing the relative signal ratio of $[1-^{13}\text{C}]\alpha\text{kV}$ or $[1-^{13}\text{C}]\alpha\text{kB}$ with $[1-^{13}\text{C}]\text{acetylcarnitine}$ (Figure 6). Furthermore, the detection of $[1-^{13}\text{C}]\alpha\text{kV}$ -hydrate in the non-pH-neutralized liquid-state experiments compared with its absence in the pH-neutralized in vivo experiment, as well as the increased signal intensity of the $[1-^{13}\text{C}]\alpha\text{kB}$ -hydrate resonance in vivo compared with the non-pH-neutralized liquid-state experiment, demonstrate the sensitivity of the proposed polarizing agents to pH and illustrate the importance of pH optimization.

The use of endogenous α kV and α kB is a potential alternative to PA as nonpersistent radical precursors. Based on the location of their natural abundance ¹³C resonances, the potential detection of pyruvate as metabolic product would not be disturbed. It is, however, a limitation of the current study that interferences of α kV and α kB with in vivo metabolic processes were not investigated. Reportedly, PDH, as well as LDH, have reduced or even absent affinities for α kB and α kV, respectively.^{41–44} This was partially confirmed in recent in vivo experiments using

hyperpolarized ^{13}C -labeled αkB that showed a decreased ^{13}C -labeling of bicarbonate compared with PA.³³ Also, αkB is converted by PDH to propionyl-CoA, avoiding any potential competing perturbation of the acetyl-CoA pool, as seen with PA.⁶ In the former study the in vitro LDH response to ^{13}C -labeled αkB varied depending on the LDH isoform.³³ While αkV is not anticipated to be appreciably converted by PDH and LDH,^{41,43,44} determining their in vivo response to hyperpolarized ^{13}C -labeled αkV , and elucidating any potential metabolic interference by it or αkB , including dose dependencies, remains to be established. Based on the aforementioned evidence of αkV not being a significant substrate of either LDH or PDH, and the lower αkV hydrate signal observed in our study, we hypothesize that αkV may be the preferred choice over αkB of nonpersistent radical precursor.

Nevertheless, radical-free dissolution DNP via the use of endogenous nonpersistent radicals provides a benefit at low cost and may increase the duration of the hyperpolarized state by avoiding one filtration step in clinical applications. In addition, UV-induced radicals of PA quench with increasing temperature¹⁸ and recombine at a threshold of 190 K,¹⁷ providing an additional benefit of UV-induced radicals in αkV and αkB to produce transportable hyperpolarized ^{13}C -labeled substrates.

5 | CONCLUSION

We conclude that the endogenous α -keto acids αkV and αkB can be used as efficient endogenous nonpersistent radicals following irradiation with UV light, achieving similar or higher ^{13}C polarization compared with PA and thus are potential candidates for translational clinical hyperpolarized MRI, enabling high polarization without requiring radical filtration. Cardiac metabolism of ^{13}C -labeled butyrate hyperpolarized with αkV or αkB demonstrated label propagation in a wide range of metabolites, demonstrating their potential as endogenous polarizing agents for in vivo radical-free hyperpolarized MRI.

ACKNOWLEDGEMENTS

We thank Thanh Lê Phong for his assistance with the microwave modulation implementation, and Analina Raquel Da Silva, Mario Lepore and Stefanita-Octavian Mitrea for their assistance with the in vivo experiments. This study was supported in part by the CIBM of the EPFL, UNIL, UNIGE, HUG and CHUV. This study was supported by funding received from the Swiss National Science Foundation (grant PZ00P3_167871 to JB, CRSK_2_190547 to AC, PZ00P2_193276 to AC), the Emma Muschamp Foundation (JB), and the Swiss Heart Foundation (grant FF18054 to JB).

ORCID

Hikari A. I. Yoshihara  <https://orcid.org/0000-0002-3274-7147>

Alice Radaelli  <https://orcid.org/0000-0002-7891-0560>

Jessica A. M. Bastiaansen  <https://orcid.org/0000-0002-5485-1308>

REFERENCES

1. Ardenkjær-Larsen JH, Fridlund B, Gram A, et al. Increase in signal-to-noise ratio of > 10,000 times in liquid-state NMR. *Proc Natl Acad Sci*. 2003; 100(18):10158-10163.
2. Golman K, Thaning M. Real-time metabolic imaging. *Proc Natl Acad Sci*. 2006;103(30):11270-11275.
3. Brindle KM. Imaging metabolism with hyperpolarized ^{13}C -labeled cell substrates. *J Am Chem Soc*. 2015;137(20):6418-6427.
4. Yoshihara HA, Bastiaansen JA, Berthonneche C, Comment A, Schwitler J. An intact small animal model of myocardial ischemia-reperfusion: Characterization of metabolic changes by hyperpolarized ^{13}C MR spectroscopy. *Am J Physiol Heart Circ Physiol*. 2015;309(12):H2058-H2066.
5. Comment A. Dissolution DNP for in vivo preclinical studies. *J Magn Reson*. 2016;264:39-48.
6. Bastiaansen JA, Merritt ME, Comment A. Measuring changes in substrate utilization in the myocardium in response to fasting using hyperpolarized [1- ^{13}C] butyrate and [1- ^{13}C] pyruvate. *Sci Rep*. 2016;6(1):1-11.
7. Nelson SJ, Kurhanewicz J, Vigneron DB, et al. Metabolic imaging of patients with prostate cancer using hyperpolarized [1- ^{13}C] pyruvate. *Sci Transl Med*. 2013;5(198):198ra108. <https://pubmed.ncbi.nlm.nih.gov/23946197/>
8. Malloy CR, Merritt ME, Dean SA. Could ^{13}C MRI assist clinical decision-making for patients with heart disease? *NMR Biomed*. 2011;24(8):973-979.
9. Cunningham CH, Lau JY, Chen AP, et al. Hyperpolarized ^{13}C metabolic MRI of the human heart: initial experience. *Circ Res*. 2016;119(11):1177-1182.
10. Aggarwal R, Vigneron DB, Kurhanewicz J. Hyperpolarized 1-[^{13}C]-pyruvate magnetic resonance imaging detects an early metabolic response to androgen ablation therapy in prostate cancer. *Eur Urol*. 2017;72(6):1028-1029.
11. Miloushev VZ, Granlund KL, Boltyanskiy R, et al. Metabolic imaging of the human brain with hyperpolarized ^{13}C pyruvate demonstrates ^{13}C lactate production in brain tumor patients. *Cancer Res*. 2018;78(14):3755-3760.
12. Cleveland ZI, Bdaiwi AS, Hossain MM, et al. Hyperpolarized ^{129}Xe diffusion MRI in cystic fibrosis lung disease: evidence for pathological alveolar enlargement. Abstract A108. *Am J Respir Crit Care Med*. 2019;199:A2568-A2568.
13. Lumata L, Merritt ME, Malloy CR, Sherry AD, Kovacs Z. Impact of Gd3+ on DNP of [1- ^{13}C] pyruvate doped with trityl OX063, BDPA, or 4-oxo-TEMPO. *J Phys Chem A*. 2012;116(21):5129-5138.
14. Yoshihara HA, Can E, Karlsson M, Lerche MH, Schwitler J, Comment A. High-field dissolution dynamic nuclear polarization of [1- ^{13}C] pyruvic acid. *Phys Chem Chem Phys*. 2016;18(18):12409-12413.

15. Ardenkjaer-Larsen JH. On the present and future of dissolution-DNP. *J Magn Reson.* 2016;264:3-12.
16. Miéville P, Ahuja P, Sarkar R, et al. Scavenging free radicals to preserve enhancement and extend relaxation times in NMR using dynamic nuclear polarization. *Angew Chem Int Ed.* 2010;49(35):6182-6185.
17. Capozzi A, Cheng T, Boero G, Roussel C, Comment A. Thermal annihilation of photo-induced radicals following dynamic nuclear polarization to produce transportable frozen hyperpolarized ¹³C-substrates. *Nat Commun.* 2017;8(1):1-7.
18. Kumada T, Noda Y, Hashimoto T, Koizumi S. Dynamic nuclear polarization study of UV-irradiated butanol for hyperpolarized liquid NMR. *J Magn Reson.* 2009;201(2):115-120.
19. Eichhorn TR, Takado Y, Salameh N, et al. Hyperpolarization without persistent radicals for in vivo real-time metabolic imaging. *Proc Natl Acad Sci.* 2013;110(45):18064-18069.
20. Capozzi A, Hyacinthe J-N, Cheng T, et al. Photoinduced nonpersistent radicals as polarizing agents for X-nuclei dissolution dynamic nuclear polarization. *J Phys Chem C.* 2015;119(39):22632-22639.
21. Bastiaansen JA, Yoshihara HA, Capozzi A, et al. Probing cardiac metabolism by hyperpolarized ¹³C MR using an exclusively endogenous substrate mixture and photo-induced nonpersistent radicals. *Magn Reson Med.* 2018;79(5):2451-2459.
22. Capozzi A, Karlsson M, Petersen JR, Lerche MH, Ardenkjaer-Larsen JH. Liquid-state ¹³C polarization of 30% through photoinduced nonpersistent radicals. *J Phys Chem C.* 2018;122(13):7432-7443.
23. Pinon AC, Capozzi A, Ardenkjaer-Larsen JH. Hyperpolarized water through dissolution dynamic nuclear polarization with UV-generated radicals. *Commun Chem.* 2020;3(1):1-9.
24. Marco-Rius I, Cheng T, Gaunt AP, et al. Photogenerated radical in phenylglyoxylic acid for in vivo hyperpolarized ¹³C MR with photosensitive metabolic substrates. *J Am Chem Soc.* 2018;140(43):14455-14463.
25. Capozzi A, Patel S, Gunnarsson CP, et al. Efficient hyperpolarization of U-¹³C-glucose using narrow-line UV-generated labile free radicals. *Angew Chem Int Ed.* 2019;58(5):1334-1339.
26. Patel S, Pinon AC, Lerche MH, Karlsson M, Capozzi A, Ardenkjaer-Larsen JH. UV-irradiated 2-keto-(1-¹³C)isocaproic acid for high-performance ¹³C hyperpolarized MR. *J Phys Chem C.* 2020;124(43):23859-23866.
27. Olson RE. Effect of pyruvate and acetoacetate on the metabolism of fatty acids by the perfused rat heart. *Nature.* 1962;195(4841):597-599.
28. Olson MS, Dennis SC, DeBuysere MS, Padma A. The regulation of pyruvate dehydrogenase in the isolated perfused rat heart. *J Biol Chem.* 1978;253(20):7369-7375.
29. Moreno KX, Sabelhaus SM, Merritt ME, Sherry AD, Malloy CR. Competition of pyruvate with physiological substrates for oxidation by the heart: implications for studies with hyperpolarized [1-¹³C] pyruvate. *Am J Physiol Heart Circ Physiol.* 2010;298(5):H1556-H1564.
30. Bastiaansen JA, Cheng T, Mishkovsky M, Duarte JM, Comment A, Gruetter R. In vivo enzymatic activity of acetylCoA synthetase in skeletal muscle revealed by ¹³C turnover from hyperpolarized [1-¹³C] acetate to [1-¹³C] acetylcarnitine. *Biochim Biophys Acta Gen Subj.* 2013;1830(8):4171-4178.
31. Ball DR, Rowlands B, Dodd MS, et al. Hyperpolarized butyrate: a metabolic probe of short chain fatty acid metabolism in the heart. *Magn Reson Med.* 2014;71(5):1663-1669.
32. Bastiaansen JA, Cheng T, Lei H, Gruetter R, Comment A. Direct noninvasive estimation of myocardial tricarboxylic acid cycle flux in vivo using hyperpolarized ¹³C magnetic resonance. *J Mol Cell Cardiol.* 2015;87:129-137.
33. von Morze C, Bok RA, Ohliger MA, Zhu Z, Vigneron DB, Kurhanewicz J. Hyperpolarized [¹³C] ketobutyrate, a molecular analog of pyruvate with modified specificity for LDH isoforms. *Magn Reson Med.* 2016;75(5):1894-1900.
34. Flori A, Giovannetti G, Santarelli MF, et al. Biomolecular imaging of ¹³C-butyrate with dissolution-DNP: Polarization enhancement and formulation for in vivo studies. *Spectrochim Acta A Mol Biomol Spectrosc.* 2018;199:153-160.
35. Abdurrachim D, Teo XQ, Woo CC, et al. Cardiac metabolic modulation upon low-carbohydrate low-protein ketogenic diet in diabetic rats studied in vivo using hyperpolarized ¹³C pyruvate, butyrate and acetoacetate probes. *Diabetes Obes Metab.* 2019;21(4):949-960.
36. Yoshihara HA, Bastiaansen JA, Karlsson M, Lerche MH, Comment A, Schwitter J. Detection of myocardial medium-chain fatty acid oxidation and tricarboxylic acid cycle activity with hyperpolarized [1-¹³C] octanoate. *NMR Biomed.* 2020;33:e4243.
37. Bastiaansen JA, Yoshihara HA, Takado Y, Gruetter R, Comment A. Hyperpolarized ¹³C lactate as a substrate for in vivo metabolic studies in skeletal muscle. *Metabolomics.* 2014;10(5):986-994.
38. Takado Y, Cheng T, Bastiaansen JA, et al. Hyperpolarized ¹³C magnetic resonance spectroscopy reveals the rate-limiting role of the blood-brain barrier in the cerebral uptake and metabolism of l-lactate in vivo. *ACS Chem Neurosci.* 2018;9(11):2554-2562.
39. Hu S, Zhu M, Yoshihara HA, et al. In vivo measurement of normal rat intracellular pyruvate and lactate levels after injection of hyperpolarized [1-¹³C] alanine. *Magn Reson Imaging.* 2011;29(8):1035-1040.
40. Wishart DS, Feunang YD, Marcu A, et al. HMDB 4.0: the human metabolome database for 2018. *Nucleic Acids Res.* 2018;46(D1):D608-D617.
41. Bremmer J. Pyruvate dehydrogenase, substrate specificity and product inhibition. *Eur J Biochem.* 1969;8(4):535-540.
42. Withycombe WA, Plummer DT, Wilkinson JH. Organ specificity and lactate-dehydrogenase activity. Differential inhibition by urea and related compounds. *Biochem J.* 1965;94(2):384-389.
43. Wilks HM, Halsall DJ, Atkinson T, Chia WN, Clarke AR, Holbrook JJ. Designs for a broad substrate specificity keto acid dehydrogenase. *Biochemistry.* 1990;29(37):8587-8591.
44. Kim MJ, Whitesides GM. L-Lactate dehydrogenase: substrate specificity and use as a catalyst in the synthesis of homochiral 2-hydroxy acids. *J Am Chem Soc.* 1988;110(9):2959-2964.
45. Cheng T, Capozzi A, Takado Y, Balzan R, Comment A. Over 35% liquid-state ¹³C polarization obtained via dissolution dynamic nuclear polarization at 7 T and 1 K using ubiquitous nitroxyl radicals. *Phys Chem Chem Phys.* 2013;15(48):20819-20822.
46. Comment A, van den Brandt B, Uffmann K, et al. Design and performance of a DNP prepolarizer coupled to a rodent MRI scanner. *Concepts Magn Reson Part B.* 2007;31(4):255-269.
47. Cheng T, Mishkovsky M, Bastiaansen JA, et al. Automated transfer and injection of hyperpolarized molecules with polarization measurement prior to in vivo NMR. *NMR Biomed.* 2013;26(11):1582-1588.
48. Shaka AJ, Keeler J, Frenkiel T, Freeman RAY. An improved sequence for broadband decoupling: WALTZ-16. *J Magn Reson.* 1983;52(2):335-338.
49. Staewen RS, Johnson AJ, Ross BD, Parrish T, Merkle H, Garwood M. 3-D FLASH imaging using a single surface coil and a new adiabatic pulse, BIR-4. *Invest Radiol.* 1990;25(5):559-567.

50. Adeva B, Arik E, Ahmad S, et al. Large enhancement of deuterium polarization with frequency modulated microwaves. *Nucl Instrum Methods Phys Res A*. 1996;372(3):339-343.
51. Hovav Y, Feintuch A, Vega S, Goldfarb D. Dynamic nuclear polarization using frequency modulation at 3.34 T. *J Magn Reson*. 2014;238:94-105.
52. Bornet A, Milani J, Vuichoud B, Linde AJP, Bodenhausen G, Jannin S. Microwave frequency modulation to enhance dissolution dynamic nuclear polarization. *Chem Phys Lett*. 2014;602:63-67.
53. Ardenkjær-Larsen JH, Bowen S, Petersen JR, et al. Cryogen-free dissolution dynamic nuclear polarization polarizer operating at 3.35 T, 6.70 T, and 10.1 T. *Magn Reson Med*. 2019;81(3):2184-2194.
54. Mishkovsky M, Anderson B, Karlsson M, et al. Measuring glucose cerebral metabolism in the healthy mouse using hyperpolarized ¹³C magnetic resonance. *Sci Rep*. 2017;7(1):1-8.

SUPPORTING INFORMATION

Additional supporting information may be found online in the Supporting Information section at the end of this article.

How to cite this article: Zanella CC, Capozzi A, Yoshihara HAI, et al. Radical-free hyperpolarized MRI using endogenously occurring pyruvate analogues and UV-induced nonpersistent radicals. *NMR in Biomedicine*. 2021;34(11):e4584. <https://doi.org/10.1002/nbm.4584>